Dalton Transactions

ROYAL SOCIETY OF CHEMISTRY

PAPER

Cite this: *Dalton Trans.*, 2022, **51**, 15996

Evaluation of the effects of newly synthesized metallophthalocyanines on breast cancer cell lines with photodynamic therapy†

Hayrani Eren Bostancı,[a] Ahmet T. Bilgiçli, *[b] Emre Güzel, [c] Armağan Günsel, [b] Ceylan Hepokur,*[a] Behzat Çimen[d] and M. Nilüfer Yarasir [b]

In this study, the new phthalonitrile derivative 3-(4-(3-oxobutyl)phenoxy)phthalonitrile (**1**) and its non-peripheral metallophthalocyanine derivatives [zinc (**2**), copper (**3**), cobalt (**4**), manganese (**5**), gallium (**6**), and indium (**7**)] were synthesized. The newly synthesized phthalocyanines were characterized by standard spectroscopic methods, such as FT-IR, ^{1}H NMR, UV-Vis, fluorescence spectroscopies, and MALDI-TOF spectrometry. Aggregation behaviors of the novel phthalocyanines were investigated by UV-Vis spectroscopy. The effect of pH change on the electronic and emission spectra of the newly synthesized phthalocyanine derivatives was studied in THF media. The electronic spectra of the new zinc (**2**), copper (**3**), and cobalt (**4**) phthalocyanines exhibited bathochromic shifts in acidic pH values due to the presence of monoprotonated forms. Surprisingly, the same effect was not observed for manganese (**5**) and indium (**7**) phthalocyanines. On the other hand, gallium (**6**) showed a slight red-shifted band with the addition of HCl to the medium. Also, it was determined that the synthesized zinc (**2**) and gallium (**6**) phthalocyanines had a selective phototoxic effect on the MCF-7 breast cancer cell line compared to the MCF-10A healthy breast cell line. The IC_{50} values of zinc (**2**) and gallium (**6**) phthalocyanines were determined for MCF-7 and MCF-10A cell lines. The IC_{50} values of MCF-7 for compounds **2** and **6** were found to be 1.721 ± 0.4 μg mL^{-1} and 7.406 ± 0.32 μg mL^{-1}, respectively. The IC_{50} values of MCF-10A for phthalocyanines **2** and **6** were found to be 48.90 ± 0.69 μg mL^{-1} and 14.77 ± 1.09 μg mL^{-1}, respectively. In the LDH (lactate dehydrogenase)-ELISA study, the LDH levels that formed on a cellular basis after the application were measured, and it was observed that the cells were directed towards apoptosis. In addition, it was observed that cancer cells underwent more apoptosis than healthy cells as a result of this application with cell-cycle and dead cell kits performed by flow cytometry. This research shows that non-peripheral substituted gallium and zinc phthalocyanine derivatives (**2** and **6**) can be suitable photosensitizers for the photodynamic treatment of breast cancers.

Received 16th June 2022,
Accepted 20th September 2022

DOI: 10.1039/d2dt01912d

rsc.li/dalton

1. Introduction

Phthalocyanines (Pcs), one of the important aromatic macrocycles, have a conjugated 18 π-electron system, and this conjugation gives it superior properties such as thermal and chemical stability. Therefore, Pcs are studied in a wide range of application areas.[1–4] One of the most important among these is medical applications due to the rapid increase in antimicrobial resistance in recent years. Thus, the synthesis and characterization of compounds used in medical applications continue to be up to date. Also, considering the superior properties of Pc molecules and the need for medical applications, it is important to synthesize and assess their potential. Recent studies have shown that Pc compounds are one of the most promising compounds for photodynamic therapy (PDT), which is being used as a new generation of cancer treatment methods.[5–7]

Cancer is one of the most important health problems today. Cancer begins with the uncontrolled proliferation of abnormal cells and can lead to death if left untreated. Cancer treatments require a multidisciplinary approach, including different options such as surgery, radiotherapy, chemotherapy, and

[a]*Department of Biochemistry, Faculty of Pharmacy, Sivas Cumhuriyet University, Sivas, Turkey. E-mail: Cozsoya@gmail.com*
[b]*Department of Chemistry, Sakarya University, Sakarya, Turkey. E-mail: abilgicli@sakarya.edu.tr; Tel: +90 264 2957116*
[c]*Department of Engineering Fundamental Sciences, Sakarya University of Applied Sciences, Sakarya, Turkey*
[d]*Department of Biochemistry, Faculty of Pharmacy, Erciyes University, Kayseri, Turkey*

† Electronic supplementary information (ESI) available. See DOI: https://doi.org/10.1039/d2dt01912d

PDT. Undesirable side effects from chemotherapy and radiotherapy have led to the research and development of different cancer treatment methods. PDT has emerged as one of these methods.[6,8,9] Although it was approved by the FDA (US Food and Drug Administration) about 30 years ago, it has not been used effectively.[10] However, especially in recent years, the effectiveness of PDT against cancer, and its use with other treatment methods, has become more important. PDT facilitates the distribution of the developed therapeutic molecule by administering it to the body and concentrating it in the cancerous area. After accumulation in the cancerous region, the developed molecule is excited by irradiating the selected region at high wavelengths, and reactive products are produced. These reactive products work as therapeutic agents by destroying the cancerous cells, enabling the removal of cancer from the patient.[11]

It is well known that different types of aggregation are observed in phthalocyanines, and are known as H- and J-type. Since it affects the photophysical and photochemical properties, the aggregation behaviors of the synthesized Pc derivatives were examined by researchers. Compared to H-type aggregation, J-type aggregation is less common.[12–14] Within the scope of this study, it was found that non-peripheral substituted Pcs with the 4-(4-hydroxyphenyl)butane-2-one group have good solubility in common organic solvents. Furthermore, their electronic spectra tend to show red-shifted bands depending on the acid being added to the medium due to the presence of the monoprotonated forms.[15,16]

In this context, 3-(4-(3-oxobutyl)phenoxy)phthalonitrile (**1**) as a new phthalonitrile derivative was synthesized. The non-peripheral metallophthalocyanine derivatives [zinc(II) (**2**), copper(II) (**3**), cobalt(II) (**4**), manganese(III) (**5**), gallium(III) (**6**), and indium(III) (**7**)] were prepared by use of this ligand. The obtained new compounds were characterized by common spectroscopic techniques. The effects of pH change on the electronic spectra of the novel types of non-peripheral metallophthalocyanine derivatives were investigated. Compounds (**2**), (**3**), and (**4**) showed clearly red-shifted bands in acidic pH values due to protonation. Furthermore, cytotoxicity studies of all compounds were performed to determine their biological activity. Many different compounds have been synthesized for photodynamic therapy studies, and studies have been carried out on different types of cancer. In this study, the effects of the newly synthesized promising Pc structures on breast cancer cell lines with photodynamic therapy were examined. Cytotoxicity tests were performed by applying the synthesized compounds on breast cancer cell lines (MCF-7) and healthy cell lines (MCF-10A). After 24 h of incubation in the dark, the death pathways of cancerous cells (*e.g.*, apoptosis, necrosis) were investigated by irradiation at high wavelengths. The results herein and the toxic effects of all phthalocyanine structures were compared with the aim to find the most suitable metallophthalocyanine structure that can be used in photodynamic therapy for breast cancer. As a result, a new therapeutic agent candidate(s) with the potential to be used in the treatment process of breast cancer with photodynamic activities will be presented.

2. Experimental

2.1. Materials and methods

The chemical substances used in the reactions and purification processes, such as 4-(4-hydroxyphenyl)butane-2-one, 3-nitrophthalonitrile, 1,8-diazabicyclo[5.4.0]undec-7-ene (DBU), K_2CO_3, methanol (MeOH), ethanol (EtOH), chloroform ($CHCl_3$), dichloromethane (CH_2Cl_2), diethyl ether, toluene, *n*-hexane, *n*-hexanol, tetrahydrofuran (THF), dimethylformamide (DMF), dimethyl sulfoxide (DMSO), $Zn(CH_3COO)_2$, $CuCl_2$, $CoCl_2$, $MnCl_2$, $GaCl_3$, and $InCl_3$ were acquired from commercial companies, such as Merck and Alfa Aesar. The purchased chemical compounds were used as received without additional purification. Electronic spectra of the novel Pcs were recorded by an Agilent Model 8453 diode array spectrophotometer. Vibrational spectra of the newly synthesized compounds were obtained by PerkinElmer spectrum two FT-IR spectrophotometers. ^{1}H NMR and ^{13}C NMR spectra were acquired by a Bruker 300 spectrometer instrument. Fluorescence spectra of related Pcs were obtained by a Hitachi S-7000 fluorescence spectrophotometer.

2.2. Synthesis

2.2.1. Synthesis of the 3-(4-(3-oxobutyl)phenoxy)phthalonitrile (1). 4-(4-Hydroxyphenyl)butane-2-one (1.04 g, 6.35 mmol) was dissolved in dry DMF (15 mL) with anhydrous K_2CO_3 (5.36 g, 38.88 mmol) in the solution. The obtained mixture was stirred for about 30 minutes under N_2 atmosphere. Then, 3-nitrophthalonitrile dissolved in DMF (1 g, 5.78 mmol) was added dropwise to the solution. This mixture was efficiently stirred under N_2 at 45 °C for three days. After completing the reaction, the obtained reaction mixture was poured into ice water (250 mL). The solid product was filtered, and washed with water and diethyl ether several times. Further purification was made by column chromatography using CH_2Cl_2 as a mobile phase. The yield of 3-(4-(3-oxobutyl)phenoxy)phthalonitrile (**1**) is 1.43 g (85%). Chemical formula: $C_{18}H_{14}N_2O_2$ (molecular weight: 290.32 g mol^{-1}). Calculated elemental analysis: C, 74.47; H, 4.86; N, 9.65; O, 11.02, found: C, 74.41; H, 4.92; N, 9.57. FT-IR (υ_{max}/cm^{-1}): 3101, 3065, 3038, 2982, 2940, 2905, 2877, 2227, 1683, 1586, 1488, 1411, 1313, 1250, 1208, 1166, 1082, 956, 852, 803, 566, 523. ^{1}H NMR (300 MHz, chloroform-*d*) δ 7.61–7.53 (m, 1H), 7.46 (dd, J = 7.7, 1.1 Hz, 1H), 7.31–7.24 (m, 2H), 7.08 (dd, J = 8.7, 1.1 Hz, 1H), 7.05–7.00 (m, 2H), 2.94 (dd, J = 8.3, 6.4 Hz, 2H), 2.81 (td, J = 7.4, 6.9, 1.7 Hz, 2H), 2.19 (s, 3H). Mass: m/z: 291.68 $[M]^+$, 329.78 $[M + K]^+$.

2.2.2. General procedure for the synthesis of phthalocyanines (2–7). The mixture of 3-(4-(3-oxobutyl)phenoxy) phthalonitrile (**1**) (0.10 g, 0.34 mmol) and the anhydrous metal salts ($Zn(CH_3COO)_2$ (16.51 mg, 0.09 mmol), $CuCl_2$ (12.15 mg, 0.09 mmol), $CoCl_2$ (11.7 mg, 0.09 mmol), $MnCl_2$ (11.34 mg, 0.09 mmol), $GaCl_3$ (15.84 mg, 0.09 mmol) or $InCl_3$ (19.9 mg, 0.09 mmol)) were heated in *n*-hexanol (2 ml) and DBU media at 150 °C under N_2 atmosphere for 8 h. After the reaction was completed, it was cooled to room temperature, and the deep green compound was precipitated with MeOH and filtered.

The obtained green-yellow Pc derivatives were washed several times with MeOH, EtOH, hexane, and diethyl ether. Column chromatography was used for further purification. Chloroform was used as a mobile phase in chromatographic purification processes. The novel synthesized Pc derivatives are soluble in common organic solvents, such as $CHCl_3$, CH_2Cl_2, THF, DMF, and DMSO.

*2.2.2.1. 1(4),8(11),15(18),22(25)-Tetrakis(4-(3-oxobutyl)phenoxy)-phthalocyaninato zinc(II) (**2**).* The phthalocyanine (**2**) yield is 0.033 g (32%). Chemical formula: $C_{72}H_{56}N_8O_8Zn$ (1226.67 g mol^{-1}). Elemental analysis: calculated; C, 70.50; H, 4.60; N, 9.13; O, 10.43; Zn, 5.33 found; C, 70.59; H, 4.56; N, 9.78. FT-IR (υ_{max}/cm^{-1}): 3065, 3031, 2954, 2919, 2856, 1711, 1600, 1502, 1474, 1432, 1361, 1243, 1201, 1160, 971, 817, 748. ^{1}H NMR (300 MHz, chloroform-*d*) δ 7.67–6.72 (m, 28H), 3.14–2.45 (m, 16H), 2.38–1.88 (m, 12H). UV-Vis (THF): λ_{max}, nm 692 (Q-band), 624 (n–π*) 326 (B-band). MS (MALDI-MS, 2,5-dihydroxybenzoic acid as matrix): 1227.98 $[M + H]^+$, 1274.85 $[M + 2Na + H]^+$.

*2.2.2.2. 1(4),8(11),15(18),22(25)-Tetrakis(4-(3-oxobutyl)phenoxy)-phthalocyaninato copper(II) (**3**).* The phthalocyanine (**3**) yield is 0.030 g (30%). Chemical formula: $C_{72}H_{56}N_8O_8Cu$ (1224.81 g mol^{-1}). Elemental analysis: calculated; C, 70.60; H, 4.61; Cu, 5.19; N, 9.15; O, 10.45, found; C, 70.98; H, 4.45; N, 9.75. FT-IR (υ_{max}/cm^{-1}): 3031, 2961, 2929, 2850, 1711, 1592, 1502, 1474, 1250, 1208, 1160, 1119, 1082, 977, 803, 740. UV-Vis (THF): λ_{max}, nm 691 (Q-band), 620 (n–π*) and 330 (B-band). MS (MALDI-MS, 2,5-dihydroxybenzoic acid as matrix): 1225.935 $[M + H]^+$, 1311.701 $[M + 2Na + K + H]^+$.

*2.2.2.3. 1(4),8(11),15(18),22(25)-Tetrakis(4-(3-oxobutyl)phenoxy)-phthalocyaninato cobalt(II) (**4**).* The phthalocyanine (**4**) yield is 0.036 g (35%). Chemical formula: $C_{72}H_{56}N_8O_8Co$ (1220.20 g mol^{-1}). Elemental analysis: calculated; C, 70.87; H, 4.63; Co, 4.83; N, 9.18; O, 10.49, found; C, 71.01; H, 4.47; N, 9.38. FT-IR (υ_{max}/cm^{-1}): 3184, 3073, 2961, 2919, 2850, 1725, 1708, 1697, 1613, 1508, 1474, 1389, 1369, 1306, 1264, 1201, 1160, 1062, 971, 824, 754. UV-Vis (THF): λ_{max}, nm 696 (Q-band), 631 (n–π*) 342 (B-band). MS (MALDI-MS, 2,5-dihydroxybenzoic acid as matrix): 1221.365 $[M + H]^+$.

*2.2.2.4. 1(4),8(11),15(18),22(25)-Tetrakis(4-(3-oxobutyl)phenoxy)-phthalocyaninato manganese(III) chloride (**5**).* The phthalocyanine (**5**) yield is 0.0040 g (38%). Chemical formula: $C_{72}H_{56}N_8O_8MnCl$ (1251.65 g mol^{-1}). Elemental analysis: calculated; C, 69.09; H, 4.51; Cl, 2.83; Mn, 4.39; N, 8.95; O, 10.23, found; C, 70.01; H, 4.56; N, 9.15. FT-IR (υ_{max}/cm^{-1}): 3038, 2954, 2905, 2877, 1711, 1586, 1502, 1480, 1327, 1243, 1201, 1160, 1118, 1062, 1013, 971, 803, 740. ^{1}H NMR (300 MHz, chloroform-*d*) δ 8.13–6.76 (m, 28H), 3.07–2.56 (m, 16H), 2.34–1.82 (m, 12H). UV-Vis (THF): λ_{max}, nm 745 (Q-band), 507 (CT), 668 (n–π*) 353 (B-band). MS (MALDI-MS, 2,5-dihydroxybenzoic acid as matrix): 1218.086 $[M - Cl + H]^+$, 1240.348 $[M - Cl + Na + H]^+$, 1252.98 $[M + H]^+$.

*2.2.2.5. 1(4),8(11),15(18),22(25)-Tetrakis(4-(3-oxobutyl)phenoxy)-phthalocyaninato gallium(III) chloride (**6**).* The phthalocyanine (**6**) yield is 0.036 g (34%). Chemical formula: $C_{72}H_{56}N_8O_8GaCl$ (1266.44 g mol^{-1}). Elemental analysis: calculated; C, 68.28; H, 4.46; Cl, 2.80; Ga, 5.51; N, 8.85; O, 10.11, found; C, 67.73; H, 4.58; N, 9.06. FT-IR (υ_{max}/cm^{-1}): 3065, 3031, 2961, 2919, 2856, 1711, 1600, 1502, 1467, 1403, 1341, 1229, 1160, 1082, 1048, 949, 824, 748. ^{1}H NMR (300 MHz, chloroform-*d*) δ 8.02–6.68 (m, 28H), 3.05–2.40 (m, 16H), 2.45–1.84 (m, 12H). UV-Vis (THF): λ_{max}, nm 711 (Q-band), 641 (n–π*) 334 (B-band). MS (MALDI-MS, 2,5-dihydroxybenzoic acid as matrix): 1231.982 $[M - Cl + H]^+$, 1267.495 $[M + H]^+$.

*2.2.2.6. 1(4),8(11),15(18),22(25)-Tetrakis(4-(3-oxobutyl)phenoxy)-phthalocyaninato indium(III) chloride (**7**).* The phthalocyanine (**7**) yield is 0.039 g (35%). Chemical formula: $C_{72}H_{56}N_8O_8InCl$ (1311.53 g mol^{-1}). Elemental analysis: calculated; C, 65.94; H, 4.30; Cl, 2.70; In, 8.75; N, 8.54; O, 9.76, found; C, 66.87; H, 4.38; N, 8.89. FT-IR (υ_{max}/cm^{-1}): 3073, 3045, 2926, 2850, 1711, 1676, 1641, 1600, 1361, 1250, 1215, 1116, 1104, 1013, 949, 796, 748. ^{1}H NMR (300 MHz, chloroform-*d*) δ 8.14–6.72 (m, 28H), 3.20–2.52 (m, 16H), 2.52–1.88 (m, 12H). UV-Vis (THF): λ_{max}, nm 714 (Q-band), 648 (n–π*) 377 (B-band). MS (MALDI-MS, 2,5-dihydroxybenzoic acid as matrix): 1277.323 $[M - Cl + H]^+$, 1312.665 $[M + H]^+$.

2.3. Fluorescence quantum yields

The fluorescence properties of the zinc, gallium, and indium Pcs were determined in THF solution at room temperature. Fluorescence quantum yields (Φ_F) of novel Pcs were calculated by the following eqn (1) in THF at room temperature.[17,18]

$$\Phi_F = \Phi_{F_{Std}} \frac{F \cdot A_{Std} \cdot \eta^2}{F_{Std} \cdot A \cdot {\eta_{Std}}^2} \quad (1)$$

In eqn (1), Φ_F is the quantum yield of the novel synthesized compounds, and Φ_F (Std) is the quantum yield of the reference compound. F and F_{Std} are the areas under the fluorescence emission curves of the novel Pcs and unsubstituted ZnPc as a standard, respectively. The absorbance of the reference and sample compounds are A_{Std} and A, respectively. n^2 and ${n_{Std}}^2$ are the refractive indices of solvents used for the sample and standard, respectively. According to the literature, the quantum yield of the used reference compound (unsubstituted ZnPc) can be defined as $\Phi_F = 0.23$ in THF.[19]

2.4. Singlet oxygen quantum yield

Singlet oxygen quantum yields of ZnPc (**2**), GaPc (**6**), and InPc (**7**) were determined by the relative method with one reference and 1,3-difenilizobenzofuran (DPBF) as a chemical quencher, using the eqn (2):

$$\Phi_\Delta = \Phi_\Delta^{Std} \frac{R \cdot I_{abs}^{Std}}{R_{Std} \cdot I_{abs}} \quad (2)$$

where Φ_Δ^{Std} is the singlet oxygen quantum yields for the standard unsubstituted ZnPc ($\Phi_\Delta^{Std} = 0.67$ in DMSO). R and R_{Std} are the DPBF photobleaching rates in the presence of the respective samples and standard, respectively. I_{abs} and I_{abs}^{Std} are the light absorption rates by the samples and standard, respectively. Solutions that contain DPBF were prepared in the dark and irradiated in the Q band region. The degradation of DPBF

at 417 nm was monitored after each 5 s irradiation.[7,20,21] The light intensity of 7.05×10^{15} photons s^{-1} cm^{-2} was used for Φ_Δ determinations. The absorption band of DPBF is reduced by light irradiation.[22–24]

2.5. Cell culture

Human epithelial breast adenocarcinoma (MCF-7) (ATCC® HTB-22™) and healthy human breast epithelial (MCF-10A) (ATCC® CRL-10317™) cells were purchased from ATCC. DMEM (with L-glutamine and $NaHCO_3$ cat. no.: D0819) medium containing 10% fetal bovine serum (FBS) (Sigma-Aldrich) and 1% penicillin–streptomycin (100 units) was used in the cell culture as the medium. Cells were incubated and multiplied at 37 °C in an incubator containing 5% CO_2 and 95% humidity. Unlike other cell lines, the MCF-10A cell line was grown by adding extra components to the medium. The cell line could be grown by adding 5% mL of horse serum, 20 ng ml^{-1} of EGF, 0.5 μg ml^{-1} of hydrocortisone, 100 ng ml^{-1} of cholera toxin, 1% penicillin–streptomycin (100 units), and 10 μg ml^{-1} of insulin into the previously prepared 500 mL medium DMEM-F12.[25] The cells were stained with Trypan blue after passage, and cell count was done with an Olympus R1 device.

2.6. Phototherapeutic application

2.6.1. Dark toxicity assay (cytotoxic effect of the photosensitizers without laser irradiation). All cells were seeded in 96-well plates at a density of approximately 2×10^4 cells per mL. Cells were allowed to attach overnight at 37 °C in a humidified atmosphere with 5% CO_2. After 24 h, the cells were incubated with various concentrations (1–100 μg ml^{-1}) of GaPc, ZnPc, InPc, MnPc and CuPc at 37 °C in a humidified atmosphere with 5% CO_2 in the dark for 2 h. A control (untreated cells) for all cells that were not exposed to any of these phthalocyanines (0 μg ml^{-1}) was included for each set of experiments. After 2 h, the photosensitized cells were washed twice with PBS and the cell viability was measured using the XTT colorimetric assay.

2.6.2. *In vitro* photodynamic therapy. For the photodynamic therapy experiments of the synthesized compounds, 2×10^4 cells were cultivated in each well. The healthy (MCF-10A) and cancer cell lines (MCF-7) were seeded in 96-well plates, and then incubated for 24 hours. All newly synthesized Pcs were dissolved in DMSO and added to the cells such that they did not exceed 2% concentration, which is a nontoxic dosage for the cells. All compounds were applied to 96-well plates at different concentrations (1–100 μg ml^{-1}) and incubated for 2 hours. Each compound was run at its concentration in 3 replicates. After 2 hours, each well was irradiated with a red diode laser (670–750 nm). A light dose of 4.5 J cm^{-2} was given to each well with a 90 mW power and 1 cm radius light source. All of these processes were carried out in a dark environment at room temperature.[26] After the application, the cell lines were incubated in a CO_2 oven for 24 hours. The compounds were then removed from the wells and washed with Phosphate Buffer Solution (PBS) five times, and the XTT (2,3-bis(2-methoxy-4-nitro-5-sulfophenyl)-5-[(phenylamino)carbonyl]-2*H*-tetrazolium hydroxide) (Cell Proliferation Assay) kit was applied. At the end of the experiment, absorbance values for each well were measured by reading at 450 nm wavelength in a microplate reader, and cell viability was calculated by taking the average absorbance values of the results studied in triplicate.

2.6.3. Flow cytometry. Flow cytometric Annexin V (apoptosis) and DNA content (cell cycle) analyses were performed with the MUSE flow cytometry device, wherein the IC_{50} results obtained were evaluated. Compounds **2** and **6** caused selective toxicity in the MCF-7 cancer cell line compared to MCF-10A. Therefore, the main pathways of compounds **2** and **6** in the cells were determined with MUSE (Annexin V) and MUSE (cell cycle) kits. Cell lines were seeded in sterile 6-well plates. After 24 hours of incubation, appropriate extract doses were given and irradiated at high wavelengths (90 mW power and 4.5 J cm^{-2} light dose). After the second incubation of 24 hours, the plate contents were removed. Cells washed with PBS were lifted with trypsin-EDTA, and centrifuged at 800 rpm for 5 min. After the obtained cells were counted with Trypan blue, 5 μL of Annexin V were added. It was incubated in the dark at room temperature for 15 min. After incubation, 400 μL of binding buffer was added to the Eppendorf tubes, and measurements were made in flow cytometry (MUSE) (emission; 530 nm, excitation; 488 nm).

2.7. LDH

The lactate dehydrogenase (LDH) molecule, which converts lactate to pyruvate during glycolysis, is a stable enzyme found in all cells. It is rapidly released into the medium upon damage to the cell membrane. An increase in the amount of dead cells or cells with damaged cell membranes results in increased LDH activity in the medium. This increase in LDH activity also causes an increase in the amount of colored formazan crystal formed at the end of the experiment, resulting in higher absorbance.[27] Following the steps in the SunRed Human (LDH) ELISA (cat. no.: 201-12-0748) kit procedure, the LDH levels formed by the cells after photodynamic therapy were measured.

2.8. Statistical analysis

Data are expressed as the mean and standard deviation ($x \pm$ SD). The ANOVA and Tukey statistical analyses were used to reveal the relationships between groups. According to the statistical programs used, the differences between the groups were considered significant for $p < 0.001$. Graph Pad 8.0 program was used in drawing the graphs, and at least three independent data were taken in the experiment.

3. Results and discussion

3.1. Synthesis and spectroscopic characterization

The starting material 3-(4-(3-oxobutyl)phenoxy)phthalonitrile (**1**) was synthesized from 4-(4-hydroxyphenyl)butane-2-one and

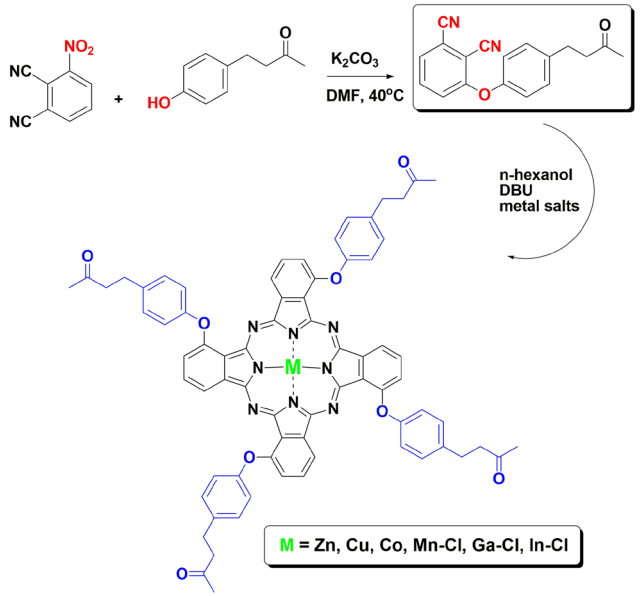

Scheme 1 The synthesis of 3-(4-(3-oxobutyl)phenoxy)phthalonitrile (**1**) and its novel type metallophthalocyanine derivatives (**2–7**).

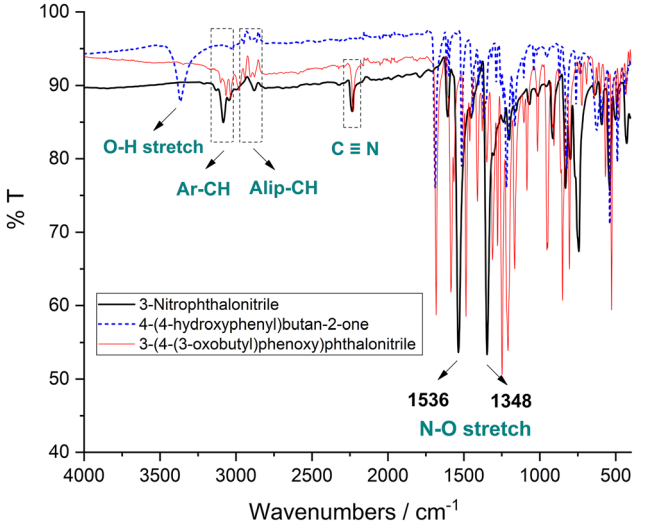

Fig. 1 FT-IR spectra of 3-nitrophthalonitrile, 4-(4-hydroxyphenyl) butan-2-one and 3-(4-(3-oxobutyl)phenoxy)phthalonitrile (**1**).

3-nitrophthalonitrile by the aromatic S_N2 substitution reaction. The synthesis of novel Pcs (**2–7**) was achieved by cyclotetramerization reaction of the new phthalonitrile derivative. The reaction was achieved by heating dry *n*-hexanol using DBU as the base and the related anhydrous metal salts ($Zn(CH_3COO)_2$ or $CuCl_2$ or $CoCl_2$, or $MnCl_2$ or $GaCl_3$ or $InCl_3$) at 150 °C in 8 h (Scheme 1). Newly synthesized 3-(4-(3-oxobutyl)phenoxy)phthalonitrile and its Pc derivatives were purified by column chromatography with CH_2Cl_2 as an eluent. After the aromatic S_N2 substitution reaction between 4-(4-hydroxyphenyl)butan-2-one and 3-nitrophthalonitrile, the nitro group peaks at 1536 cm^{-1} and 1348 cm^{-1} disappeared, and the one related to the C≡N vibration was shifted from 2234 cm^{-1} to 2227 cm^{-1}. Aromatic peaks between 3200–3000 cm^{-1} and aliphatic peaks between 3000–2800 cm^{-1} were observed (Fig. 1). After the synthesis of novel type Pcs by the cyclotetramerization reaction, the C≡N vibrational peak at 2227 cm^{-1} of compound (**1**) disappeared. The FTIR spectra of all metallophthalocyanine derivatives (**2–7**) are very similar, except for small stretching shifts (Fig. S1†).

UV-Vis spectroscopy is a simple and beneficial technique for the characterization of Pcs due to the extended conjugated π-system. It is well known that Pcs have characteristic peaks in electronic spectra, which are called the Q-band and the B-band. The Q-band appears at 650–700 nm due to the π–π* transition, while the B-band appears at 300–400 nm due to the deeper π–π* transition. In addition, the fact that the Q band is single or double gives clues about whether the Pcs are metal or metal-free.[28] The electronic spectra of novel Pcs were recorded in THF at room temperature using the Agilent Model 8453 diode array spectrophotometer. The Q-band absorption values of the novel type non-peripheral Pc derivatives (**2–7**) appeared at 692 nm, 691 nm, 696 nm, 745 nm, 711 nm, and 714 nm, respectively (Table 1 and Fig. 2). When these values were compared with the substituted Pcs from their peripheral positions, they were found to be about 20 nm red-shifted as expected.[7,29] The B-band values of the non-peripheral Pc derivatives (**2–7**) in electronic spectra were observed at 326 nm, 330 nm, 342 nm, 353 nm, 334 nm, and 377 nm, respectively (Table 1 and Fig. 2). Pcs are versatile building blocks in material production due to their delocalized π-electronic structure. Their conjugation properties and ability to form macrocyclic compounds with many metal ions provide them with fascinating physical properties. They can show different colors even according to the atom in the center. Fig. 3 shows the colors of the solutions prepared in THF of the synthesized compounds. The color differences occur with the change of transition metal atoms in the center. This color change is consistent with the electronic spectra of the newly synthesized Pc derivatives. NMR spectroscopy was also used to characterize the structures of the synthesized compounds. The NMR spectra of the compounds were taken in a deuterated dimethyl sulfoxide (d_6-DMSO) solution. The aromatic and aliphatic protons for 3-(4-(3-oxobutyl)phenoxy)phthalonitrile (**1**) confirmed the expected structure (Fig. S2†). In the ^1H NMR spectra of diamagnetic phthalocyanines, the protons in the aromatic region could be obtained broadly due to the π–π interactions in high concentrations. ^1H NMR spectra of Pcs (**3**) and (**4**) could not be obtained due to the paramagnetic properties of the structures containing Cu^{2+} and Co^{2+} ions in the phthalocyanine ring.[18,30] MALDI-TOF mass spectrometry has been used to characterization of the Pcs. The protonated or sodium and potassium adduct peaks of the newly synthesized Pcs were observed in the mass spectra (Fig. S4–S8†).

Table 1 Spectral parameters and photophysical properties (Φ_F) of novel synthesized metallophthalocyanines (**2–7**) in THF

	Absorbance			Fluorescence				
Pcs	λ^{abs}_{max} (nm) (Q-band)	λ^{abs}_{max} (nm) (B-band)	λ^{abs}_{max} (nm) (n–π*)	λ^{em}_{max} (nm) (emission)	λ^{exc}_{max} (nm) (excitation)	$\Delta\lambda$ (nm) (Stokes shift)	Φ_F, % (quantum yield)	Φ_Δ (singlet oxygen)
2	692	326	624	708	693	16	0.18	0.92
3	691	330	620	—	—	—	—	—
4	696	342	631	—	—	—	—	—
5	745	353	668	—	—	—	—	—
6	711	334	641	728	708	17	0.09	0.56
7	714	377	648	732	715	14	0.11	0.72
ZnPc[a]	666	342		673	666	7	0.23	0.67
GaPc[b]	680			691	680	11	0.30	0.41
InPc[b]	686			700	689	14	0.018	0.67

[a] From ref. 17. [b] From ref. 22.

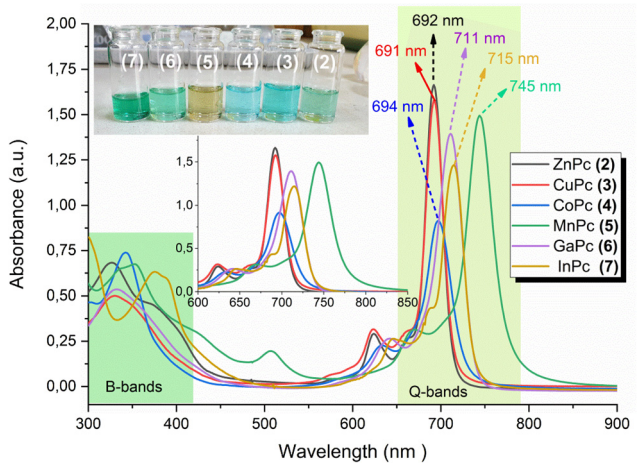

Fig. 2 UV-Vis spectra of novel synthesized phthalocyanines (**2–7**) in THF (inset: the region of the electronic spectra between 600 nm and 850 nm).

3.2. Aggregation studies

In Pcs, aggregation formation reduces the solubility and its effectiveness as a photosensitizer. Therefore, aggregation has a negative effect on its biological properties. The main reason for the aggregation of Pcs is their high π-conjugation systems. However, the addition of bulky functional groups to their peripheral or non-peripheral locations can prevent or reduce their aggregation tendency. Based on this information, the aggregation behaviors of the new non-peripheral substituted Pcs were investigated in the solvent medium. For this purpose, electronic spectra of Pcs at different concentrations were recorded by UV-Vis spectroscopy. As the concentration increased, the intensity of the Q-bands at 692 nm for (**2**) (Fig. 4a), 691 nm for (**3**) (Fig. S9†), 696 nm for (**4**) (Fig. S10†), 745 nm for (**5**) (Fig. S11†), 711 nm for (**6**) (Fig. S12†), and 714 nm for (**7**) (Fig. S13†) increased, and no new band formation was observed due to aggregation. The increase of the Q-band with concentration behaved following the Lambert–Beer law. *R*-Squared values of synthesized Pc derivatives (**2–6**) were calculated at about 0.99 for all compounds.

3.3. Fluorescence properties

Fluorescence properties of the novel synthesized ZnPc (**2**), GaPc (**6**), and InPc (**7**) were investigated in THF at room temperature, and the obtained results are summarized in Table 1. Fluorescence emission peaks of Pcs (**2**, **6**, and **7**) were observed at 708 nm for (**2**), 728 nm for (**6**), and 732 nm for (**7**) (Fig. 4b for **2**, Fig. 4c for **6**, and Fig. 4d for **7**). Fig. 4 shows that the absorption and excitation spectra are similar. The similarity in the absorption and excitation spectra of wavelength for Pcs **2**, **6**,

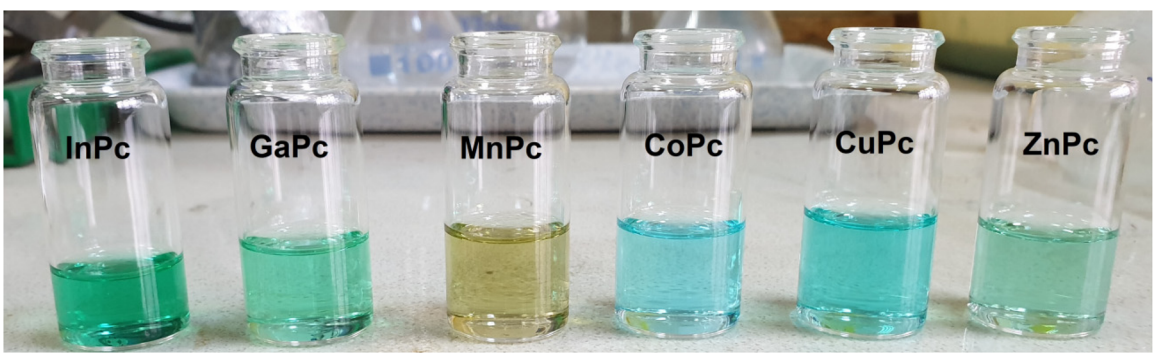

Fig. 3 Digital photograph of phthalocyanine solutions (**2–6**) in THF media.

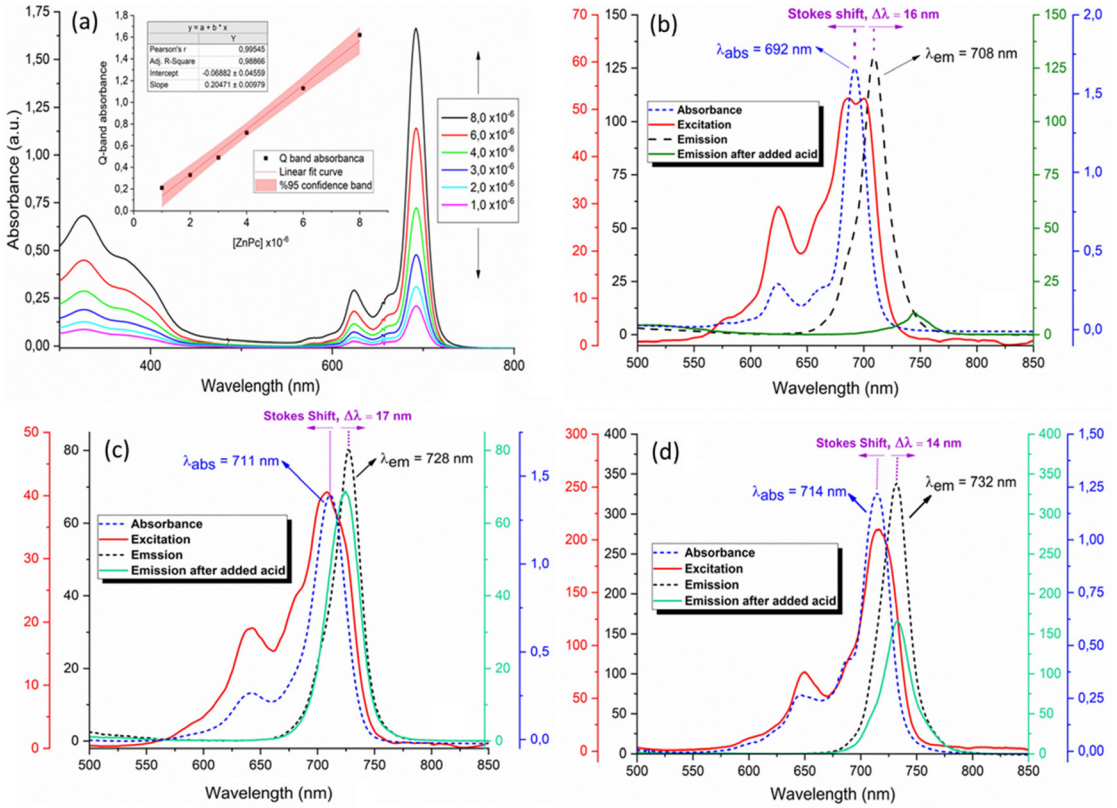

Fig. 4 (a) Electronic spectra of ZnPc (**2**) at different concentrations in THF (inset: Q-band absorbance *versus* concentration). (b) Absorbance, excitation, and emission spectra of ZnPc (**2**) and the change of the emission spectra after the addition of acid (λ_{ex} = 661 nm). (c) Absorbance, excitation, and emission spectra of GaPc (**6**) and the change of the emission spectra after the addition of acid (λ_{ex} = 680 nm). (d) Absorbance, excitation, and emission spectra of InPc (**7**) and the change of the emission spectra after the addition of acid (λ_{ex} = 685 nm).

and **7** indicates that the nuclear configurations of the excited state and ground state are not affected in THF due to excitation. In addition, the emission spectra of the novel Pcs are the mirror image of the excitation spectrum. The Stokes shift values of these compounds were found to be 16 nm for **2**, 17 nm for **6**, and 14 nm for **7** (Table 1). The fluorescence quantum yield and Stokes shift values of ZnPc (**2**), InPc (**5**), and GaPc (**6**) are consistent with the literature.[22] Fluorescence quantum yields (Φ_F) for ZnPc (**2**), GaPc (**6**), and InPc (**7**) were found to be 0.18, 0.09, and 0.11, respectively (Table 1). The quantum yield for ZnPc (**2**) is lower than that for the unsubstituted ZnPc in THF.[31] This value shows that the non-peripheral substitution of Pcs with 4-(4-hydroxyphenyl)butane-2-one groups caused the reduction of the fluorescence quantum yield.[7] Moreover, for GaPc (**6**) and InPc (**7**), the fluorescence quantum yields are lower than those for ZnPc (**2**) and unsubstituted gallium or indium Pc due to the heavier atom effect in these Pc derivatives. The heavy atoms caused a decrease in quantum yield due to the enhancement of intersystem crossing.[32]

3.4. The effect of pH change upon the UV-Vis and fluorescence spectra of phthalocyanines

The change of the UV-Vis and fluorescent spectra of synthesized Pcs was also investigated by the titration of HCl. For this, HCl solutions were prepared at a concentration of 10^{-3} M. Pcs were prepared at a concentration of 10^{-5} M in THF–H_2O (9 : 1 v/v). After the stepwise addition of 10 μL acid solutions to the Pc solutions, the electronic spectra of the mixtures were recorded, and the pH of the solution was measured with the help of a pH meter. The newly synthesized phthalocyanine derivatives had characteristic Q- and B-bands as expected in electronic spectra. However, the addition of HCl caused red-shifted bands for ZnPc (**2**) (Fig. 5), CuPc (**3**) (Fig. 6), and CoPc (**4**) (Fig. 7), while the same effect was not observed for MnPc (Fig. S14†), GaPc (Fig. S15†) and InPc (Fig. S16†). The maximum absorption peaks of ZnPc (**2**), CuPc (**3**), and CoPc (**4**) at 692, 691, and 696 nm, respectively, gradually decreased with increasing pH towards acidic values, and new peaks formed at 741, 745, and 756 nm in the red-shifted region. This indicates that the electronic spectra of ZnPc (**2**), CuPc (**3**), and CoPc (**4**) are sensitive to pH changes. In particular, ZnPc (**2**) showed very high sensitivity to pH change when compared to the other Pcs. A small change in pH caused severe changes in the electronic spectrum for ZnPc (**2**). Therefore, it has the potential to be used as a pH sensor. The difference in pH also caused significant changes in the fluorescence emission spectrum of ZnPc (**2**). The approach of pH towards acidic values caused quenching of the emission peak at 721 nm and a shift

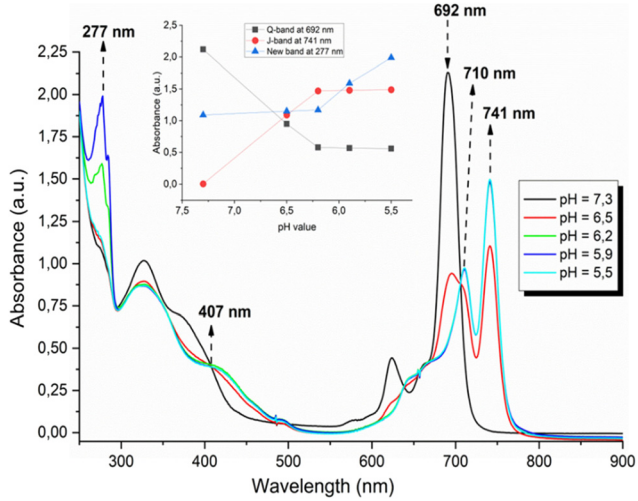

Fig. 5 UV-Vis spectra of ZnPc (**2**) at different pH values (inset: the change of the Q-band and J-band absorbance *versus* pH value).

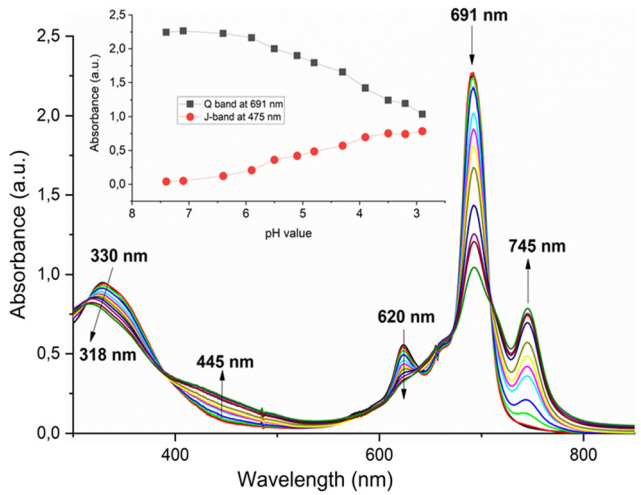

Fig. 6 UV-Vis spectra of CuPc (**3**) at different pH values (inset: the change of the Q-band and J-band absorbance *versus* pH value).

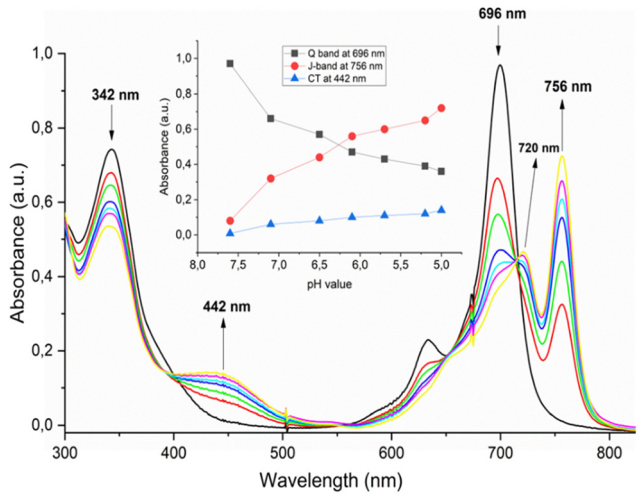

Fig. 7 UV-Vis spectra of CoPc (**4**) at different pH values (inset: the change of the Q-band and J-band absorbance *versus* pH value).

towards 744 nm (Fig. 4b). The emission spectra of GaPc (**6**) and InPc (**7**) were not significantly affected by pH change. Only some decrease in emission intensity at 728 nm for **6** and 732 nm for **7** were observed by bringing the pH from 7–8 to acidic values (Fig. 4c for **6** and Fig. 4d for **7**).

3.5. Singlet oxygen generation measurements

PDT is a cancer treatment method that uses singlet oxygen produced by a photosensitizer to destroy tumor cells. Pcs are widely studied as photosensitive compounds for PDT applications due to their high singlet oxygen generating capacity. In PDT, the molecule, which is sensitive to light, is first excited to the singlet state and then turns to the triplet state with the intersystem transition. It contributes to singlet oxygen production by transferring the light-sensitive molecular energy in the triplet state to the ground state oxygen. The singlet oxygen produced acts as a cytotoxic species for cancer cells, and kills tumor cells by type II mechanism.[33] The amount of singlet oxygen produced by the photosensitive material is found by calculating the singlet oxygen quantum yield (Φ_Δ). The Φ_Δ values of the newly synthesized ZnPc (**2**), GaPc (**6**), and InPc (**7**) were investigated in DMSO at room temperature. For singlet oxygen quantum yield measurements, ZnPc (**2**), GaPc (**6**), and InPc (**7**) were dissolved in DMSO. 1,3-Diphenylisobenzofuran (DPBF) was used as the quenching agent. UV-Vis spectra of the solution exposed to light at 5-second intervals were recorded. Changes in absorption at 417 nm of DPBF were examined (Fig. 8 for **2**, Fig. S17† for **6**, and Fig. S18† for **7**). Since DPBF is a light-sensitive compound, care was taken to keep the solution in a dark environment. During the Φ_Δ determinations, the intensity of the Q-band, characteristic of Pc molecules, did not change significantly, even remaining at nearly the same intensity. This shows us that the compounds do not degrade during singlet oxygen studies. The Φ_Δ values of non-peripheral phthalocyanine derivatives containing 4-(4-hydroxyphenyl) butane-2-one groups were found to be 0.91 for ZnPc (**2**), 0.56

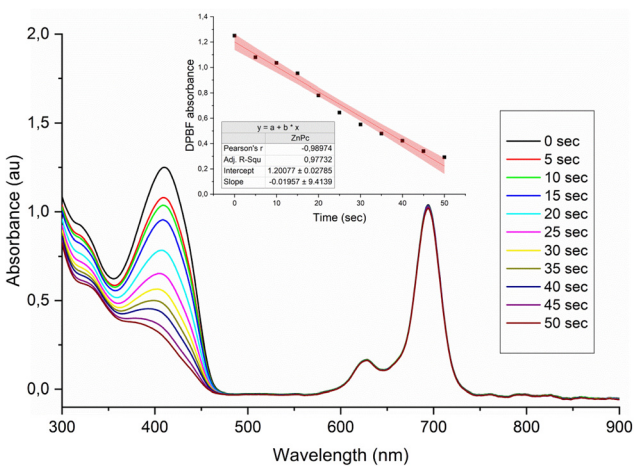

Fig. 8 Absorption changes of ZnPc (**2**) during the determination of the singlet oxygen quantum yield in DMSO (inset: plot of DPBF absorbance *vs.* time).

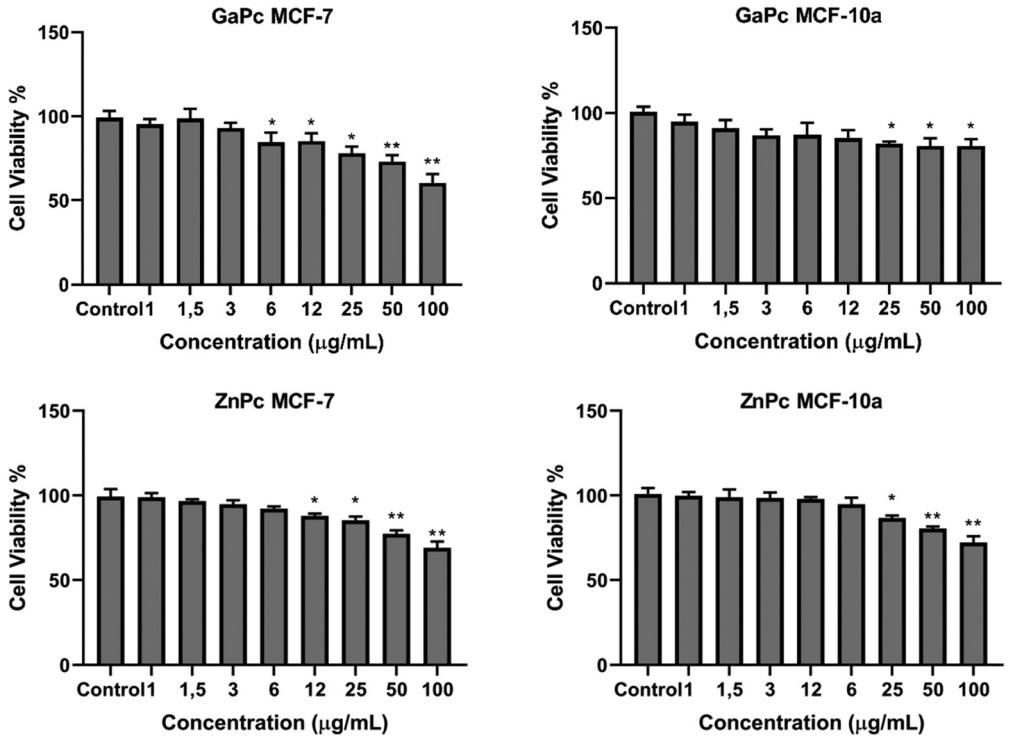

Fig. 9 The cell viability (%) of MCF-7 and MCF-10A cells with different concentrations of GaPc (**6**) and ZnPc (**2**) for without laser treatment (*: $p < 0.001$, **: $p < 0.0001$).

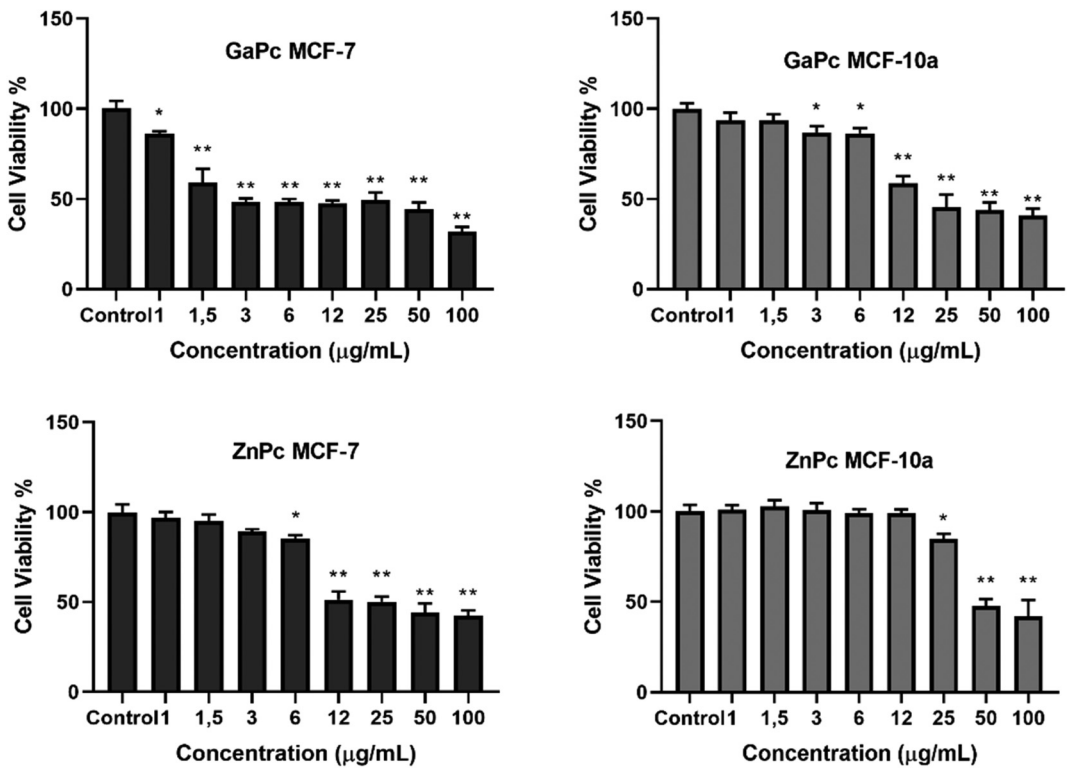

Fig. 10 The cell viability (%) of MCF-7 and MCF-10A cells with different concentrations of GaPc (**6**) and ZnPc (**2**) for with laser treatment (*: $p < 0.001$, **: $p < 0.0001$).

for GaPc (**6**) and 0.72 for InPc (**7**). In general, it can be said that the synthesized non-peripheral substituted zinc, gallium, and indium Pc derivatives (**2**, **6**, and **7**) are suitable for PDT applications as they produce reasonably high singlet oxygen yields.

3.6. Dark toxicity

The effects of all newly synthesized compounds on cell viability at different concentrations as a result of dark toxicity tests were investigated. As a result, it was determined that ZnPc (**2**) and GaPc (**6**) were not toxic without irradiation. The results obtained for these two compounds are shown in Fig. 9. Since other structures have toxic effects on healthy and cancer cell lines without irradiation, they were not studied in the next steps.

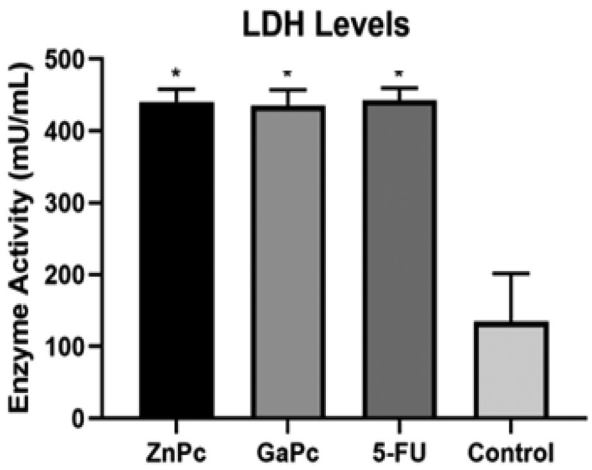

Fig. 11 LDH enzyme activity values of ZnPc (**2**) and GaPc (**6**) on MCF-7 cells.

3.7. Cell culture

The IC_{50} doses of the synthesized Pcs were determined by the XTT method, and the obtained data were calculated with the Graph Pad 8.0 program. In this direction, the statistical relationships of the IC_{50} values were evaluated and interpreted with Tukey's multiple comparison test in the GraphPad 8.0 program. When the statistical data were examined, the data between MCF-10A and MCF-7 cells given ZnPc (**2**) and the data between MCF-10A and MCF-7 cells given GaPc (**6**) were found to be significant ($p < 0.0001$). MCF-10A treated with ZnPc (**2**) had an IC_{50} of 48.90 ± 0.69 μg mL^{-1}, while the IC_{50} value of MCF-7 was 7.406 ± 0.32 μg mL^{-1}. The IC_{50} value of MCF-10A administered with GaPc (**6**) was 14.77 ± 1.09 μg mL^{-1}, while the IC_{50} value of MCF-7 was 1.721 ± 0.4 μg mL^{-1}. With these results, the effects of ZnPc (**2**) and GaPc (**6**) synthesis on MCF-10A and MCF-7 cells were investigated in the next stages of the study (Fig. 10).

3.8. LDH enzyme activity

When the activity results were examined, a significant increase was observed in the cell lines given ZnPc (**2**) and GaPc (**6**) compared to the LDH level in the MCF-7 cell line, which was not treated. Statistically, there is a significant increase in the cell lines in which the newly synthesized Pcs were given compared to the living cells ($p < 0.0001$). However, 5-FU (fluorouracil), which is used in cancer treatment, was used as a positive control. Agreement was found in the LDH levels in the MCF-7 cell lines to which this drug was applied and that for the cell lines where the new synthesis structures were applied (Fig. 11).

3.9. Flow cytometry

In healthy cells, one of the membrane lipids, phosphatidylserine (PS), is present on the cytoplasmic surface of the cell membrane. If the cell undergoes apoptosis, PS molecules that are normally located on the inner surface are translocated to the outer surface of the cell membrane. This displacement

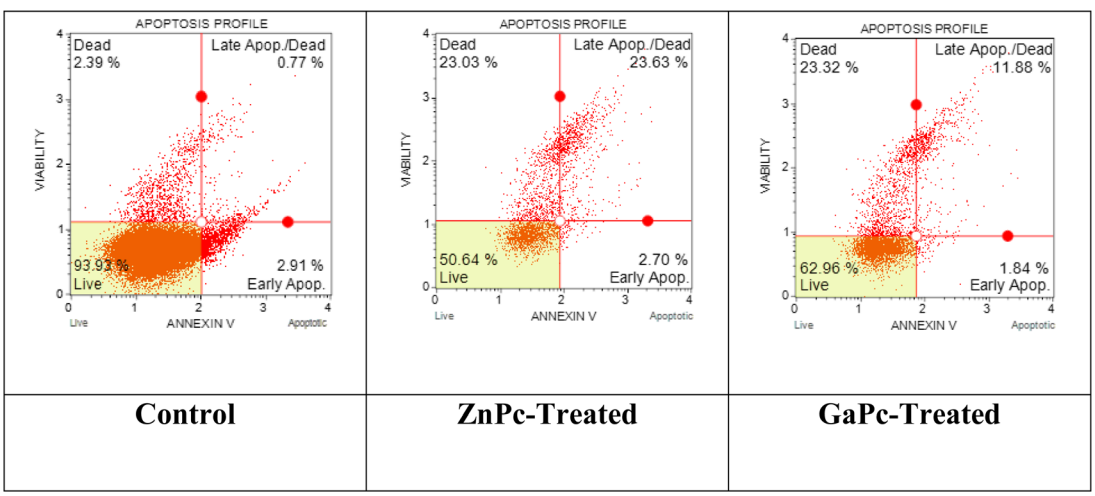

Fig. 12 Flow cytometry results of ZnPc (**2**) and GaPc (**6**) against the MCF-7 cell line with irradiation.

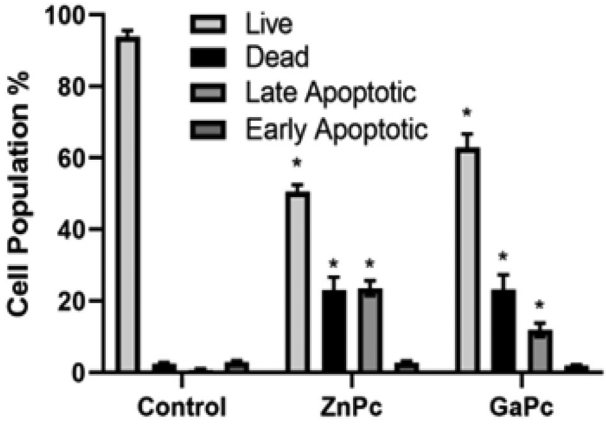

Fig. 13 The death cells resulting from the interaction of MCF-7 cells with ZnPc (**2**) and GaPc (**6**).

occurs early in apoptotic cell death when the cell membrane integrity is not compromised. Since Annexin V is a protein that can bind to phosphatidylserine translocated to the cell's outer surface, the apoptotic cell can be made visible by labeling it with a fluorescent substance (*e.g.*, FITC).[34] In ineffective cancer drugs, the drug kills the cell by causing apoptosis.[35] Therefore, an increase in the apoptosis/necrosis ratio indicates that the drug's efficacy is increased (Fig. 12). When the results obtained from the molecules studied in this study were examined, it was seen that the rate was high. As a result of the study, it can be seen that Pcs **2** and **6** have a toxic effect on the MCF-7 cancer cell line after irradiation (Fig. 13).

3.10. Cell cycle

According to the obtained cell cycle analysis results, it was observed that the cell cycle was significantly stopped in the G0/G1 phase ($p < 0.0001$) in the MCF-7 cell line stimulated at a high wavelength after administration of ZnPc (**2**) and GaPc (**6**) (Fig. 14 for **2** and Fig. 15 for **6**).

3.11. Evaluation of breast cancer cell lines results

Currently, studies on the development of Pcs are continuing in the field of PDT due to their strong effects on the tissue and their absorbance properties at high wavelengths.[36] The most important feature desired in photosensitive structures is strong absorbance at high wavelengths (650–750 nm) with the aim to reach all cancer cells with PDT by affecting the tissue deeply. In addition, photosensitive structures are required to show stable properties.[37] It is well known that metallophthalocyanine complexes have highly stable structures.[38] The dark toxicity tests demonstrated that only two of the newly synthesized compounds (ZnPc (**2**) and GaPc (**6**)) given without irradiation did not show toxic properties in both cancer and normal cell lines, and studies on these structures continued. Likewise, ZnPc (**2**) and GaPc (**6**) are effective in killing this cancer cell line. In line with this study, IC_{50} doses under 4.5 J cm^{-2} light dose were applied to the breast cancer cell

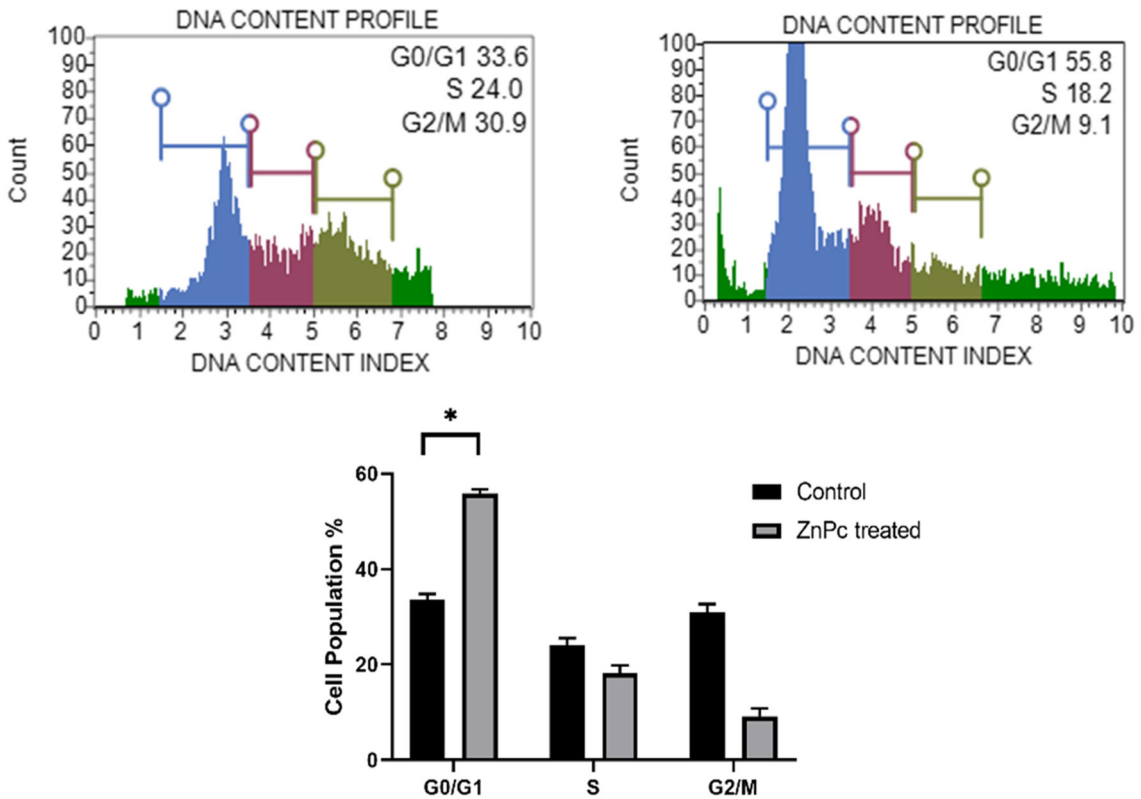

Fig. 14 Cell cycle graphs of MCF-7 cells before and after photodynamic therapy with ZnPc (**2**).

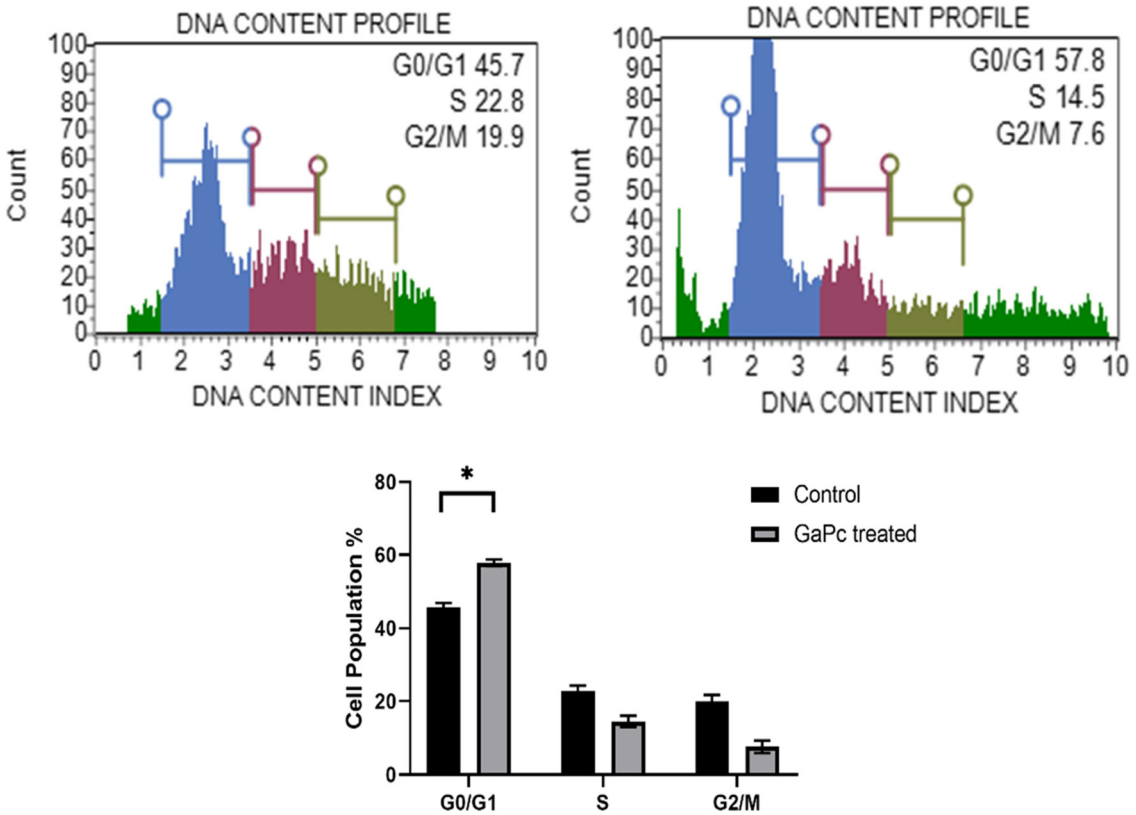

Fig. 15 Cell cycle graphs of MCF-7 cells before and after photodynamic therapy with GaPc (**6**).

lines, and the effects were observed. In our study, we observed that ZnPc (**2**) and GaPc (**6**) were more effective on the MCF-7 cell line when IC_{50} doses were applied.

Since other compounds (CuPc (**3**), CoPc (**4**), MnPc (**5**), InPc (**7**)) exhibited toxic properties without irradiation, studies on these compounds were discontinued. In line with the IC_{50} results obtained, lower values were obtained for the MCF-7 cell line compared to the MCF-10A cell line.

In our study, no difference was observed between the IC_{50} doses of ZnPc (**2**) and GaPc (**6**) against the positive control (5-FU), but a significant increase in the LDH enzyme was observed against the negative control. George *et al.*[27] used Rubus extract and phthalocyanine structures together on breast cancer cell lines. As a result, they observed apoptotic cell death in cancer cells, and also decreased ATP proliferation and increased LDH enzyme. George *et al.* stated that Annexin V/PI results showed apoptosis-induced cell death by the PDT. These values are given in Section 3.7. Data obtained as a result of flow cytometry also showed a tendency toward apoptosis in cancer cells after irradiation (Fig. 12). These results support the data in our study.

4. Conclusions

In the present study, 3-(4-(3-oxobutyl)phenoxy)phthalonitrile (**1**) and its non-peripheral Pc derivatives (**2**–**7**) were successfully prepared. The novel synthesized Pcs are not aggregated in solution media. The synthesized ZnPc (**2**), CuPc (**3**), and CoPc (**4**) showed red-shifted bands in acidic pH values. In particular, ZnPc (**2**) has a very high sensitivity to pH change when compared to the other Pcs. A small change in pH causes severe changes in the electronic spectrum of ZnPc (**2**). Therefore, it has the potential to be used as a pH sensor. The electronic spectra of MnPc (**5**), GaPc (**6**), and InPc (**7**) are not sensitive to pH changes. Furthermore, the potential of ZnPc, GaPc and InPc (**2**, **6** and **7**) as photosensitizers in photodynamic therapy was assessed on the basis of measuring various photochemical and photophysical properties. The effects of the newly synthesized ZnPc (**2**) and GaPc (**6**) on breast cancer cell lines by photodynamic therapy were also investigated. The results show that the ZnPc (**2**) and GaPc (**6**) structures were effective on the MCF-7 cell line. By applying the examples in the aforementioned studies, it is predicted that these structures can be made more easily accessible to the target cancer tissue by applying different coating methods, and they have a high potential to be used in breast cancer as an effective cancer treatment method.

Conflicts of interest

There are no conflicts to declare.

References

1 P. C. Lo, M. S. Rodríguez-Morgade, R. K. Pandey, D. K. P. Ng, T. Torres and F. Dumoulin, *Chem. Soc. Rev.*, 2020, **49**, 1041–1056.
2 C. G. Claessens, U. Hahn and T. Torres, *Chem. Rec.*, 2008, **8**, 75–97.
3 B. Yıldız, E. Güzel, D. Akyüz, B. S. Arslan, A. Koca and M. K. Şener, *Sol. Energy*, 2019, **191**, 654–662.
4 A. Günsel, E. Kırbaç, B. Tüzün, A. Erdoğmuş, A. T. Bilgiçli and M. N. Yarasir, *J. Mol. Struct.*, 2019, **1180**, 127–138.
5 M. Wysocki, B. Czarczynska-Goslinska, D. Ziental, M. Michalak, E. Güzel and L. Sobotta, *ChemMedChem*, 2022, **17**, e202200185.
6 B. De Zheng, Q. X. He, X. Li, J. Yoon and J. D. Huang, *Coord. Chem. Rev.*, 2021, **426**, 213548.
7 A. Günsel, E. Güzel, A. T. Bilgiçli, G. Y. Atmaca, A. Erdoğmuş and M. N. Yarasir, *J. Lumin.*, 2017, **192**, 888–892.
8 B. De Zheng, S. L. Li, Z. L. Huang, L. Zhang, H. Liu, B. Y. Zheng, M. R. Ke and J. D. Huang, *J. Photochem. Photobiol., B*, 2020, **213**, 112086.
9 B. Y. Zheng, L. Wang, Q. Y. Hu, J. Shi, M. R. Ke and J. D. Huang, *Dyes Pigm.*, 2020, **177**, 108286.
10 P. Agostinis, K. Berg, K. A. Cengel, T. H. Foster, A. W. Girotti, S. O. Gollnick, S. M. Hahn, M. R. Hamblin, A. Juzeniene, D. Kessel, M. Korbelik, J. Moan, P. Mroz, D. Nowis, J. Piette, B. C. Wilson and J. Golab, *Ca-Cancer J. Clin.*, 2011, **61**, 250–281.
11 W. Li, Y. N. Sun, X. T. Yan, S. Y. Yang, E. J. Kim, H. K. Kang and Y. H. Kim, *J. Agric. Food Chem.*, 2013, **61**, 10730–10740.
12 Y. C. Yang, J. R. Ward and R. P. Seiders, *Inorg. Chem.*, 1985, **24**, 1765–1769.
13 E. J. Osburn, L. K. Chau, S. Y. Chen, N. Collins, D. F. O'Brien and N. R. Armstrong, *Langmuir*, 1996, **12**, 4784–4796.
14 F. Bächle, C. Maichle-Mössmer and T. Ziegler, *ChemPlusChem*, 2019, **84**, 1081–1093.
15 A. T. Bilgiçli, T. Kandemir, B. Tüzün, R. Arıduru, A. Günsel, Ç. Abak, M. N. Yarasir and G. Arabaci, *Appl. Organomet. Chem.*, 2021, e6353.
16 M.-J. Lin, X. Fang, M.-B. Xu and J.-D. Wang, *Spectrochim. Acta, Part A*, 2008, **71**, 1188–1192.
17 A. T. Bilgiçli, H. Genç Bilgiçli, A. Günsel, H. Pişkin, B. Tüzün, M. Nilüfer Yarasir and M. Zengin, *J. Photochem. Photobiol., A*, 2020, **389**, 112287.
18 A. Günsel, A. T. Bilgiçli, B. Tüzün, H. Pişkin, M. N. Yarasir and B. Gündüz, *New J. Chem.*, 2019, **44**, 369–380.
19 E. T. Saka, M. Durmuş and H. Kantekin, *J. Organomet. Chem.*, 2011, **696**, 913–924.
20 E. Güzel, A. Günsel, A. T. Bilgiçli, G. Y. Atmaca, A. Erdoğmuş and M. N. Yarasir, *Inorg. Chim. Acta*, 2017, **467**, 169–176.
21 E. Kirbaç, G. Y. Atmaca and A. Erdoğmuş, *J. Organomet. Chem.*, 2014, **752**, 115–122.
22 E. Güzel, *RSC Adv.*, 2019, **9**, 10854–10864.
23 I. Gürol, M. Durmuş, V. Ahsen and T. Nyokong, *Dalton Trans.*, 2007, 3782–3791.
24 M. Durmuş and V. Ahsen, *J. Inorg. Biochem.*, 2010, **104**, 297–309.
25 J. Debnath, S. K. Muthuswamy and J. S. Brugge, *Methods*, 2003, **30**, 256–268.
26 K. Maduray and B. Odhav, *J. Photochem. Photobiol., B*, 2013, **128**, 58–63.
27 B. P. George, H. Abrahamse and N. M. Hemmaragala, *Photodiagn. Photodyn. Ther.*, 2017, **19**, 266–273.
28 E. Güzel, M. N. Yarasir and A. R. Özkaya, *Synth. Met.*, 2020, **262**, 116331.
29 A. T. Bilgiçli, A. Günsel, M. Kandaz and A. R. Özkaya, *Dalton Trans.*, 2012, **41**, 7047–7056.
30 M. S. Ağırtaş, B. Cabir, Ü. Yıldıko, S. Özdemir and S. Gonca, *Chem. Pap.*, 2020, **1**, 3.
31 E. Kırbaç and A. Erdoğmuş, *J. Mol. Struct.*, 2020, **1202**, 127392.
32 V. Chauke, M. Durmuş and T. Nyokong, *J. Photochem. Photobiol., A*, 2007, **192**, 179–187.
33 M. Durmuş, Photochemical and Photophysical Characterization, in *Photosensitizers in Medicine, Environment, and Security*, ed. T. Nyokong and V. Ahsen, Springer, Dordrecht, 2011.
34 D. L. Bratton, V. A. Fadok, D. A. Richter, J. M. Kailey, L. A. Guthrie and P. M. Henson, *J. Biol. Chem.*, 1997, **272**, 26159–26165.
35 C. P. Baines, *Front. Physiol.*, 2010, **1**, 156.
36 X. Zhang, N. Kobayashi and J. Jiang, *Spectrochim. Acta, Part A*, 2006, **64**, 526–531.
37 J. Vara, M. S. Gualdesi, S. G. Bertolotti and C. S. Ortiz, *J. Mol. Struct.*, 2019, **1181**, 1–7.
38 Y. Zhang and J. F. Lovell, *Wiley Interdiscip. Rev.: Nanomed. Nanobiotechnol.*, 2017, **9**, e1420.